Biophysical Journal Volume 105 November 2013 2427–2436

Adsorption and Distribution of Fluorescent Solutes near the Articular Surface of Mechanically Injured Cartilage

Sarah G. A. Decker, Mohammad Moeini, Hooi Chuan Chin, Derek H. Rosenzweig, and Thomas M. Quinn*

Department of Chemical Engineering, McGill University, Montreal, QC, Canada

ABSTRACT The development of cartilage-specific imaging agents supports the improvement of tissue assessment by minimally invasive means. Techniques for highlighting cartilage surface damage in clinical images could provide for sensitive indications of posttraumatic injury and early stage osteoarthritis. Previous studies in our laboratory have demonstrated that fluorescent solutes interact with cartilage surfaces strongly enough to affect measurement of their partition coefficients within the tissue bulk. In this study, these findings were extended by examining solute adsorption and distribution near the articular surface of mechanically injured cartilage. Using viable cartilage explants injured by an established protocol, solute distributions near the articular surface of three commonly used fluorophores (fluorescein isothiocyanate (FITC), tetramethylrhodamine isothiocyanate (TRITC), and carboxytetramethylrhodamine (TAMRA)) were observed after absorption and subsequent desorption to assess solute-specific matrix interactions and reversibility. Both absorption and desorption processes demonstrated a trend of significantly less solute adsorption at surfaces of fissures compared to adjacent intact surfaces of damaged explants or surfaces of uninjured explants. After adsorption, normalized mean surface intensities of fissured surfaces of injured explants were 6%, 40%, and 32% for FITC, TRITC, and TAMRA, respectively, compared to uninjured surfaces. Similar values were found for sliced explants and after a desorption process. After desorption, a trend of increased solute adsorption at the site of intact damaged surfaces was noted (316% and 238% for injured and sliced explants exposed to FITC). Surface adsorption of solute was strongest for FITC and weakest for TAMRA; no solutes negatively affected cell viability. Results support the development of imaging agents that highlight distinct differences between fissured and intact cartilage surfaces.

INTRODUCTION

Articular cartilage is a specialized soft tissue, which is imperative to the function of synovial joints by permitting the smooth movement of load-bearing surfaces (1). Injury or degeneration of this tissue results in significant joint pain and a loss of mobility (2,3). Cartilage injury can arise from joint trauma and may worsen during progression of osteoarthritis, a degenerative joint disease affecting millions (4). Cartilage has limited capabilities of self-repair and therefore injury can eventually lead to complete degradation of the tissue. The initial stage of injury is generally characterized by surface fissures or fibrillation and biochemical changes in the extracellular matrix (ECM) involving glycosaminoglycan (GAG) and water content (5–7). The detection of these changes at the earliest possible stage is beneficial for effective treatment (8).

Minimally invasive imaging techniques such as delayed gadolinium-enhanced magnetic resonance imaging of cartilage (9–11) and contrast-enhanced computed tomography (12–14) are of interest in part due to their abilities to quantify GAG content. These methods involve the use of readily available contrast agents, generally anionic, which diffuse into cartilage and experience electrostatic repulsion from negatively charged matrix GAGs. This leads to an inverse relationship between contrast agent concentration and GAG density (15). A major drawback of these methods is the high concentration of contrast agent required to obtain acceptable images due to the repulsive interactions experienced (16). Recent studies have exploited these electrostatic interactions by examining the use of positively charged contrast agents to improve imaging and GAG quantification at lower concentrations (17–19). Although promising results have been observed, maximum attenuation values were not reached until near equilibrium conditions. Generally in clinical practice, diffusion takes place over a limited period of time and these conditions are likely not met. To overcome this limitation, other studies have investigated the use of contrast agent diffusion rates rather than equilibrium distribution for functional assessment of cartilage (20,21).

The development of imaging techniques based on detection of surface damage, also an early stage indicator of cartilage injury, could provide another potential tool for cartilage integrity assessment. However, interactions between solutes and cartilage surfaces have received only limited attention and are not well characterized or understood. Previous studies have been mostly focused on lubricating molecules, which bind or adsorb to the articular surface such as proteoglycan-4, albumin, γ-globulin, and surface-active phospholipids (22–26). Other previous work has investigated the adsorption of a wide range of solutes to cartilage surfaces and its effect on bulk partition coefficient measurements (27).

The aim of this study was to examine solute adsorption and distribution near the articular surface of mechanically injured cartilage for potential use in cartilage integrity assessment. Three commonly used fluorophores were

Submitted March 20, 2013, and accepted for publication September 4, 2013.

*Correspondence: thomas.quinn@mcgill.ca

Editor: Peter Hunter.

0006-3495/13/11/2427/10 $2.00

http://dx.doi.org/10.1016/j.bpj.2013.09.037

studied and a method of quantification was developed to allow for comparison of solute adsorption to healthy versus damaged cartilage surfaces. It was hypothesized that significant differences in adsorption intensity would be linked to structural and biochemical changes due to injury and associated fissures. Findings may suggest new, to our knowledge, possibilities for development of imaging agents based on detection of surface fibrillation or fissuring.

MATERIALS AND METHODS

Osteochondral explants

Adult bovine knees (skeletally mature) were obtained fresh from a local slaughterhouse and visually healthy osteochondral cores, 8 mm in diameter, were drilled perpendicular to the articular surface of the distal femur using a power drill and coring bit (Snug-Plug Cutters, Veritas Tools, Ottawa, Canada) (Fig. 1 *A*) and then placed in 25 mL of sterile phosphate buffered saline (PBS) containing antibiotic/antimycotic solution (Life Technologies, Burlington, Canada). The cartilage of these cylindrical explants was trimmed to 2.5 mm diameter using a biopsy punch (Miltex, York, PA) and scalpel. Trimmed samples were then incubated in chondrocyte culture medium (high-glucose DMEM containing 0.1 mM nonessential amino acids, 10 mM HEPES, 10% fetal bovine serum, and 1% penicillin-streptomycin-glycine solution; Life Technologies) for 1–2 days before experimentation.

Mechanical injury

Osteochondral explants were subjected to radially unconfined axial compression within a precision mechanical loading apparatus consisting of a load cell (model 31, Honeywell, Golden Valley, MN) and displacement actuator (LTA-HL, Newport, Irvine, CA) mounted in an aluminum and stainless steel frame interfaced with virtual instrumentation software (LabVIEW, National Instruments, Austin, TX). To induce injury, a single compressive ramp at 0.7 s^{-1} strain rate and 14 MPa peak stress was applied as determined by previous studies (28,29). The high strain rate loading from this protocol was reported to cause surface fissures in ~90% of cases, tissue swelling, and GAG loss (28,30,31). Explants were then placed into absorption baths (below).

Sliced positive controls for injury-induced fissures

The mechanical injury protocol has been found to introduce fissures that are ~200 μm deep (21). For comparison purposes, positive controls were created by slicing the articular surface of uninjured explants to a depth of 200 μm. This slicing involved a vertical cut across the diameter of the cartilage surface using a vibrating blade microtome (VT1200S, Leica Microsystems GmbH, Wetzlar, Germany). Samples were then placed into absorption baths (below).

Solutes

Three fluorescent solutes were used in this study: fluorescein isothiocyanate (FITC), tetramethylrhodamine isothiocyanate (TRITC) (Sigma-Aldrich, St. Louis, MO), and carboxytetramethylrhodamine (TAMRA) (Life Technologies). These solutes are relatively small rigid molecules with similar molecular masses (389, 443, and 430 Da, respectively) but different electric charges (FITC is negatively charged in solution, whereas TRITC and TAMRA are positively charged) and slightly different structures (27). These three commonly used fluorophores provide a good starting point for investigation of solute adsorption to articular cartilage surfaces. They are readily detected in imaging experiments, and although they may not be immediately applicable clinically, their chemistry and physical properties are well known so that custom-made solutes for cartilage imaging could be made to mimic their properties. Stock solutions were prepared to a concentration of 250 μM in culture medium and were filtered through a 0.2 μm syringe filter (Sigma-Aldrich) to eliminate solid particles or bacterial contaminants.

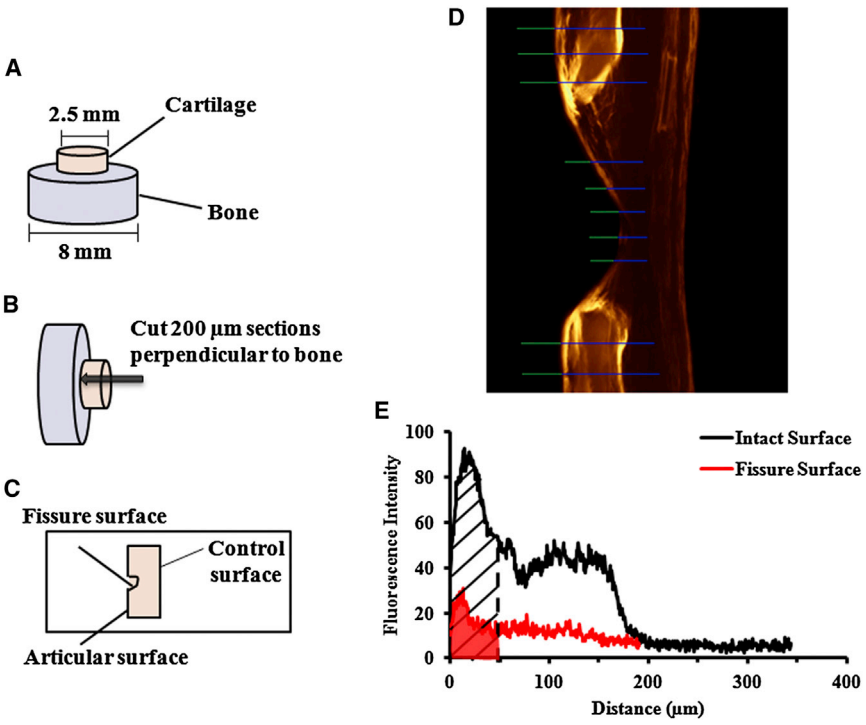

FIGURE 1 Osteochondral cores (*A*) were equilibrated with absorption baths and subsequent desorption baths. 200 μm thick sections were then cut through the cartilage depth perpendicular to the bone (*B*) and placed on a microscope slide to be imaged by fluorescence microscopy (*C*). Fluorescent images were analyzed by taking the mean of 5 linescans (*D*) and quantifying the area under the 50 μm of the resulting intensity versus distance plot (*E*) using a composite Simpson's rule. To see this figure in color, go online.

Absorption/desorption baths

Solute adsorption to cartilage surfaces was examined under two conditions: directly after an absorption process and after an absorption-desorption process. Each set of experiments used nine joints in total from different cows taking place over a period of 3 weeks. Each week, explants were harvested from three joints and then mixed and randomly sorted into three experimental groups (uninjured, injured, and sliced) such that each group contained 16–22 explants. Absorption baths were prepared to a fluorescent solute concentration of 7.5 μM in culture medium. Cartilage explants (both bone and cartilage) were placed in the baths and left to equilibrate in the incubator for a period of 18–20 h. For experiments that involved the added desorption step, explants were then removed from absorption baths and placed into new baths of culture medium (initially free of fluorescent solute) and once again left to equilibrate in the incubator for 18–20 h.

Visual assessment and quantification of solute adsorption

Cartilage explants were removed from baths (absorption or desorption) and mounted on the vibrating blade microtome such that the blade was perpendicular to the cartilage surface. 200 μm thick sections were cut through the cartilage and detached from the bone using a scalpel (Fig. 1 *B*). The sections were then placed on a microscope slide with the articular surface oriented toward the left and the cut surface (deep zone cartilage) acting as a control edge (not exposed directly to the bath; Fig. 1 *C*). Fluorescence intensity images were acquired using an inverted fluorescence microscope (IX81, Olympus America, Center Valley, PA). Fluorescence microscopy has a known source of error associated with the contribution of fluorescence intensity from regions above and below the focal depth, which may fluoresce enough to create noise in the image. To remove any bias associated with this error, a series of images was taken from top to bottom of the sample and the same image number was analyzed for each sample.

To quantify images obtained from fluorescence microscopy, a method was derived that gave a good representation of the surface fluorescence intensity and allowed for comparison of intensities between injury conditions. At various points along the surface, linescans that provided fluorescence intensity measurements every 0.645 μm were taken from the articular surface into the tissue. At the same points, a second linescan was taken extending past the articular surface away from the tissue to measure the background intensity, which was subtracted from the overall intensity. An average of five linescans per sample image was taken on both the intact and cracked surfaces to give a good representation of the entire surface (Fig. 1 *D*). This provided a plot of fluorescence intensity versus distance and a composite Simpson's rule was used to approximate the area under the first 50 μm of these curves (Fig. 1 *E*). The mean of all six samples was then obtained as the overall surface intensity for each solute under each condition and represented as a plot of intensity versus distance.

Solute partitioning measurements

Effective partition coefficients of solutes were measured using absorption-desorption processes. For each solute, cartilage explants (2.5 mm in diameter) were obtained from three different joints and distributed randomly into the three experimental groups (uninjured, injured, and sliced) such that each group contained 15–18 explants. Explants were sectioned to 500 μm thickness with a microtome (VT 1200, Leica Microsystems GmbH, Wetzlar, Germany) with inclusion of the articular surface intact and allowed to equilibrate with 400 μL absorption baths of 50 μM FITC, 15 μM TRITC, and 15 μM TAMRA for 20 h. Following equilibration, explants were removed from absorption baths and surface fluid was removed gently with a tissue, and the explants were then placed in 150 μL desorption baths of culture medium (initially free from solute) and left to equilibrate again for 20 h. All processes were carried out in the incubator. Equilibrium fluorescence intensities of absorption and desorption baths were measured using the plate reader (Mithras LB940, Berthold Technologies GmbH & Co. KG, Bad Wildbad, Germany) as a measure of solute concentration. Pilot studies using standard chondroitin sulfate solutions (in PBS) confirmed linear calibrations between fluorescence intensities and solute concentrations. Explant wet weights were measured using an analytical balance (AL204, Mettler Toledo, Mississauga, Canada). Explants were then lyophilized (FreeZone 2.5, Labconco, Kansas City, MO) and weighed dry. The difference between wet and dry weights provided total explant fluid content.

The solute effective partition coefficient K was defined as the ratio of solute concentration within the cartilage fluid to that within surrounding bath. K was determined from conservation of solute in the desorption bath (32):

$$K = \frac{c_d V_d}{V_f (c_a - c_d)}, \tag{1}$$

where c_a and c_d represent the equilibrium adsorption and desorption bath solute concentrations, V_d is desorption bath volume, and V_f is explant fluid volume. K is termed the effective partition coefficient as it may include several factors specific to the geometry and experimental conditions, such as solute-matrix interactions, tissue inhomogeneity, and surface adsorption.

Explant GAG measurements

The lyophilized explants (from the partitioning experiments) were digested overnight at 60°C in a solution of PBS containing 0.01% sodium azide, 5 mM cysteine-HCl, and 125 μg/mL papain (Sigma-Aldrich). Explant GAG contents were then determined colorimetrically using the dimethylmethylene blue spectrophotometric method (33).

Quantification of cell viability

After an absorption-desorption process (following the same procedure as described previously), uninjured explants were sectioned using the vibrating blade microtome as described previously. A LIVE/DEAD assay kit was used according to manufacturer's instructions (Life Technologies) (29). Samples were visualized on an Olympus IX81 inverted fluorescence microscope. All images were captured using a 10× objective with MAG Biosystems Software 7.5 (Photometrics, Tucson, AZ). Three random positions per slide were captured from three independent experiments ($n = 9$). Positively stained nuclei were counted and plotted as a percent of total nuclei.

Statistical analysis

Significant differences among fluorescence intensities of uninjured surfaces and injured or sliced surfaces were identified using the Student's t-test. Differences among solutes in partition coefficient (K), explant GAG and fluid contents, adsorption strengths, and cell viability were identified using analysis of variance and Tukey post hoc tests. Values are reported as Mean ± SE. Results were considered significant for $p < 0.05$.

RESULTS

Surface accumulation of solute after absorption

Visual assessment of microscope images of FITC, TRITC, and TAMRA clearly showed fissures in injured and sliced explants and obvious differences between damaged explants (injured or sliced) and uninjured cartilage (Fig. 2). Sections of uninjured explants showed an intense fluorescence signal at the articular surface, which became less intense and more

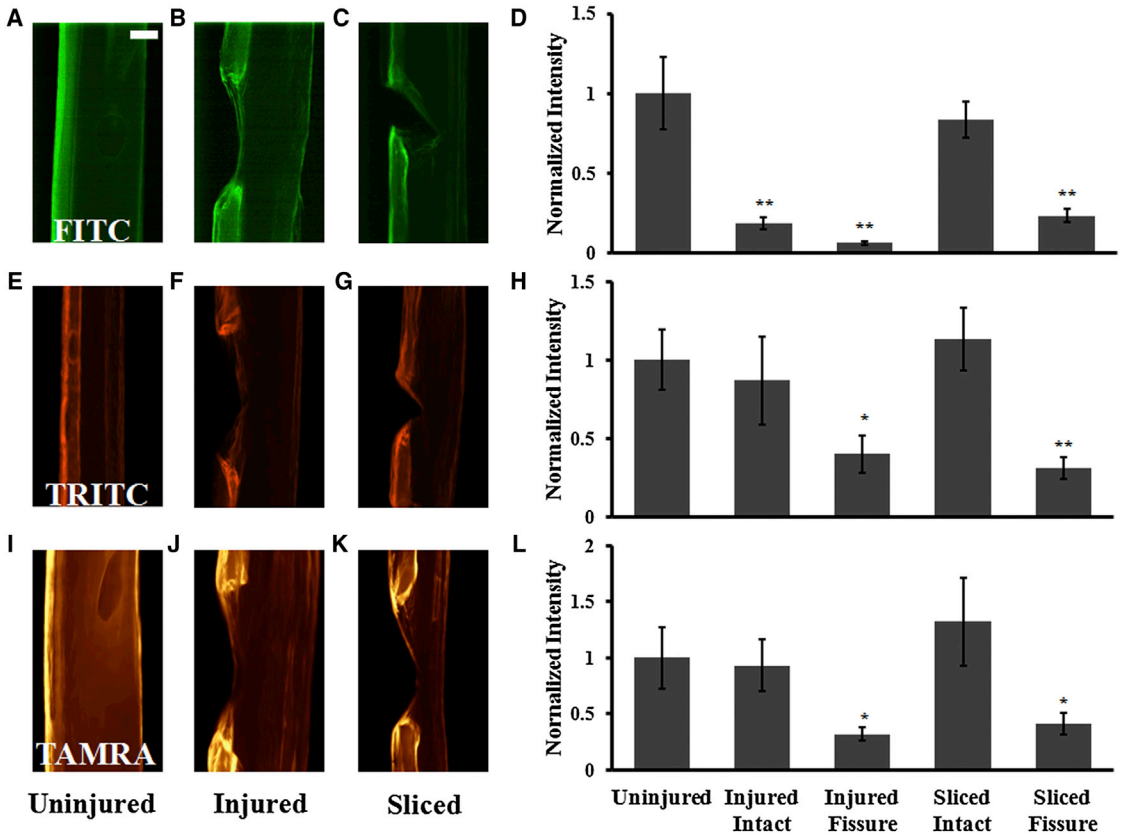

FIGURE 2 Fluorescence microscope images of uninjured (*A*, *E*, *I*), injured (*B*, *F*, *J*), and sliced (*C*, *G*, *K*) sections of cartilage explants equilibrated with FITC (*A*, *B*, *C*), TRITC (*E*, *F*, *G*), or TAMRA (*I*, *J*, *K*). Bar graphs represent normalized mean intensity of fluorescence within the first 50 μm from the surface for FITC (*D*), TRITC (*H*), and TAMRA (*L*). Significance represents comparison of damaged explant surfaces to uninjured explant surfaces. Mean $\pm$ SE ($n = 6$); * $= p < 0.05$; ** $= p < 0.01$. Scale bar is 200 μm. To see this figure in color, go online.

uniformly distributed deeper within the cartilage through to the control edge (Fig. 2, *A*, *E*, and *I*). The control edge was not in direct contact with the bath; therefore, the relatively weak fluorescence signal likely reflected partitioning of solute within the bulk of the tissue. Injured and sliced explants showed a strong fluorescence signal at the intact articular surface; however, it became noticeably weaker at sites of fissures even though the surfaces within the fissures had been directly exposed to the bath (Fig. 2, *B*, *C*, *F*, *G*, *J*, and *K*). Fluorescence intensity at fissure sites appeared to be only marginally stronger than deeper within the tissue. Fluorescence intensity deep within the tissue was similar between uninjured, injured, and sliced explants.

For injured and sliced explants, mean fluorescence intensity within the first 50 μm depth from the surface in contact with the bath was normalized to that of uninjured explants (Fig. 2, *D*, *H*, and *L*). Statistical comparisons were made for all intact and fissured surfaces within injured and sliced explants to the surface of uninjured explants. For all solutes, these surface fluorescence intensities were not significantly different between intact surfaces of injured or sliced explants and surfaces of uninjured explants with the exception of the intact surface of injured explants exposed to FITC, where the normalized mean intensity was 18% ($p < 0.01$). All solutes showed a significant decrease in intensity between the fissured surfaces of injured and sliced explants and the surface of uninjured explants. For fissures in injured explants, normalized mean surface intensities were 6% ($p < 0.01$), 40% ($p < 0.05$), and 32% ($p < 0.05$) for FITC (Fig. 2 *D*), TRITC (Fig. 2 *H*), and TAMRA (Fig. 2 *L*), respectively. For fissures in sliced explants, normalized mean surface intensities were 23% ($p < 0.01$), 31% ($p < 0.01$), and 41% ($p < 0.05$) for FITC, TRITC, and TAMRA, respectively.

Surface accumulation of solute after desorption

Microscope images of FITC, TRITC, and TAMRA after desorption (Fig. 3) were similar to those obtained after absorption, albeit with less overall intensity. Fluorescence intensities of intact surfaces of injured and sliced explants exposed to FITC were significantly higher than fluorescence intensities of surfaces of uninjured explants, having normalized mean intensities of 316% ($p < 0.01$) and 238% ($p < 0.01$), respectively (Fig. 3 *D*). Normalized mean intensity of fissured surfaces was only significantly different from uninjured controls for injured explants at 43% ($p < 0.01$), but approached significance for sliced explants ($p < 0.07$) (Fig. 3 *D*). For explants exposed to TRITC, intact surfaces

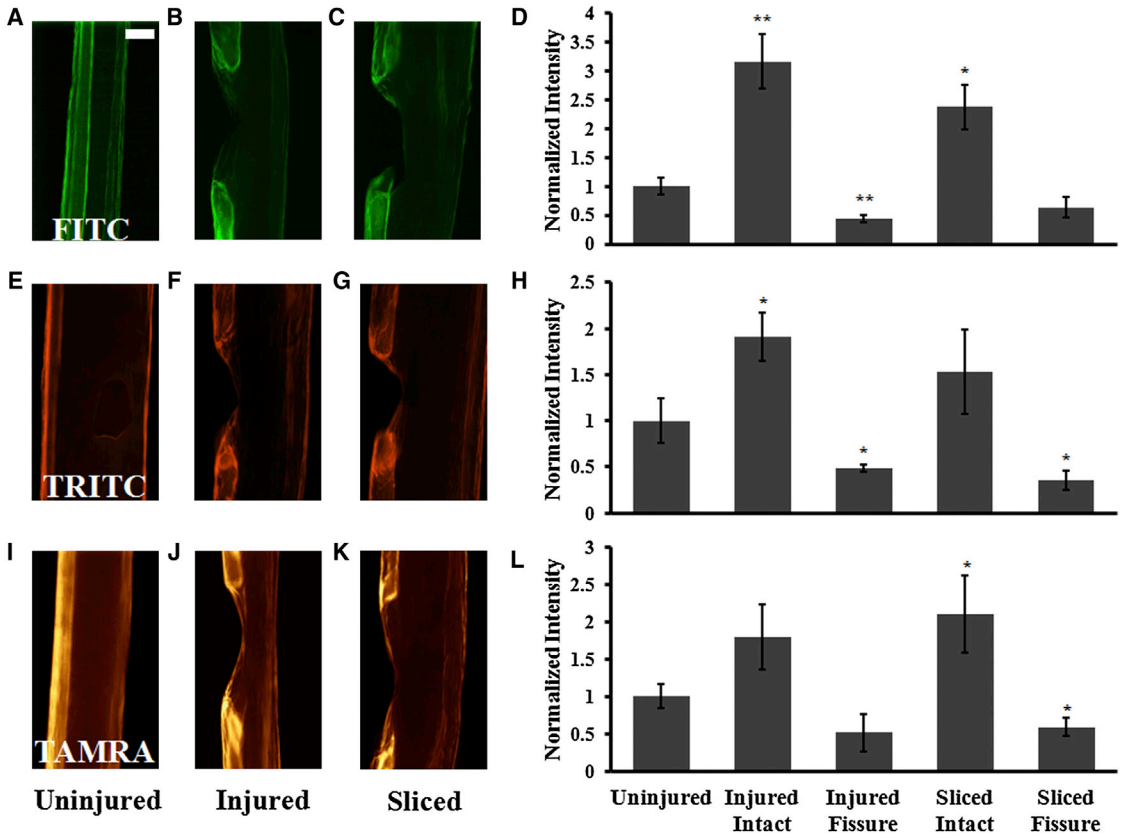

FIGURE 3 Fluorescence microscope images of uninjured (*A*, *E*, *I*), injured (*B*, *F*, *J*), and sliced (*C*, *G*, *K*) sections of cartilage explants equilibrated with desorption baths of culture media initially free from fluorescent solute after equilibration with FITC (*A*, *B*,*C*), TRITC (*E*, *F*, *G*), or TAMRA (*I*, *J*, *K*). Bar graphs represent normalized mean intensity of fluorescence within the first 50 μm from the surface for FITC (*D*), TRITC (*H*), and TAMRA (*L*). Significance represents comparison of damaged explant surfaces to uninjured explant surfaces. Mean $\pm$ SE ($n = 6$); * = $p < 0.05$; ** = $p < 0.01$. Scale bar is 200 μm. To see this figure in color, go online.

of injured explants had a significantly higher normalized mean intensity of 191% ($p < 0.05$), whereas fissured surfaces of injured and sliced explants had fluorescence intensities significantly less than uninjured explants with normalized mean intensities of 49% ($p < 0.05$) and 36% ($p < 0.05$), respectively (Fig. 3 *H*). For explants exposed to TAMRA, only surfaces of sliced explants exhibited significant differences from surfaces of uninjured controls with normalized mean intensities of 209% ($p < 0.05$) for intact surfaces and 59% ($p < 0.05$) for fissured surfaces. Normalized mean intensities of the intact and fissured surface of injured explants approached significance with $p < 0.06$ and $p < 0.07$, respectively (Fig. 3 *L*).

Fissured-to-intact surface intensity ratios for injured and sliced explants

Within individual damaged explants (injured or sliced), fluorescence intensity within the first 50 μm depth from fissured surfaces in contact with the bath were normalized to adjacent intact surfaces, resulting in a mean intensity ratio. Statistical comparisons were made between the mean intensity ratio of damaged explants and a theoretical intensity ratio of 1 for surfaces of uninjured explants. After absorption, intensity ratios of injured and sliced explants were found to be significantly less than one ($p < 0.001$) for all solutes (Fig. 4, *A*, *B*, and *C*). Similar results were obtained for intensity ratios of injured and sliced explants after desorption ($p < 0.001$) for all solutes (Fig. 4, *D*, *E*, and *F*).

Solute adsorption strengths and effects on cell viability

Adsorption strengths were estimated from uninjured controls by dividing the fluorescence intensity after desorption by the fluorescence intensity after absorption for each solute. Results showed that FITC adsorbed most strongly, whereas TAMRA adsorbed most weakly. FITC and TAMRA differed significantly from one another ($p < 0.01$) however TRITC did not differ significantly from either (Fig. 5). Cell viability was not significantly affected by the fluorescent solutes used in this study; samples exposed to FITC, TRITC, and TAMRA had 77%, 80%, and 71% viable cells, which was similar to previous control findings (29) (results not shown).

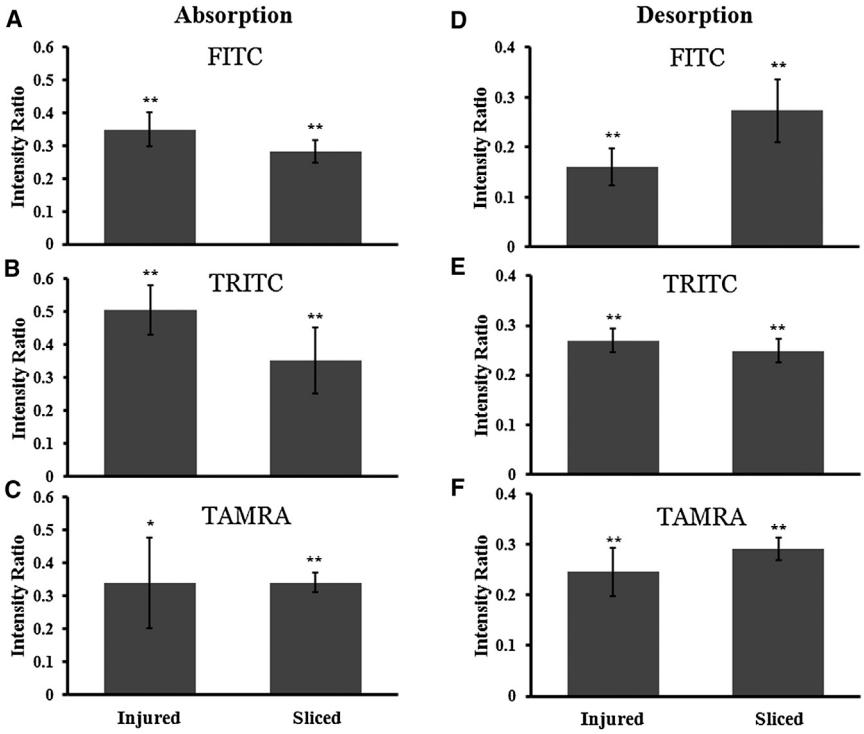

FIGURE 4 Mean ratio of fissure surface fluorescence intensity normalized to intact surface fluorescence intensity within individual injured and sliced explants after absorption (*A*, *B*, *C*) and subsequent desorption (*D*, *E*, *F*) for FITC (*A*, *D*), TRITC (*B*, *E*), and TAMRA (*C*, *F*). Statistical comparisons were made to a theoretical ratio of 1 for uninjured cartilage surface. Mean ± SE ($n = 6$); * = $p < 0.05$; ** = $p < 0.001$.

Effect of mechanical injury on solute effective partition coefficients and explant GAG and fluid content

Effective partition coefficients for uninjured explants were found to be 0.54 ± 0.026, 2.82 ± 0.21, and 2.54 ± 0.16 for FITC, TRITC, and TAMRA, respectively. *K* for injured explants was found to be 0.61 ± 0.056, 2.4 ± 0.17, and 2.3 ± 0.057 for FITC, TRITC, and TAMRA, respectively. *K* for sliced explants was found to be 0.52 ± 0.028, 2.57 ± 0.14, and 2.32 ± 0.035 FITC, TRITC, and TAMRA, respectively. Mechanically injured and sliced explants exhibited no significant differences in overall mean effective partition coefficients (*K*) versus uninjured control explants for all solutes (Fig. 6 *A*). There was also no significant difference between *K* of injured explants and sliced explants. *K* varied between solutes, with partitioning of FITC being significantly less than that of TRITC or TAMRA for all experimental conditions ($p < 0.01$). Explant GAG and fluid contents were not significantly affected by mechanical injury versus control explants, with no significant differences between injured and sliced explants (Fig. 6, *B* and *C*). Similarly, no differences in explant GAG and fluid contents were detected between explants.

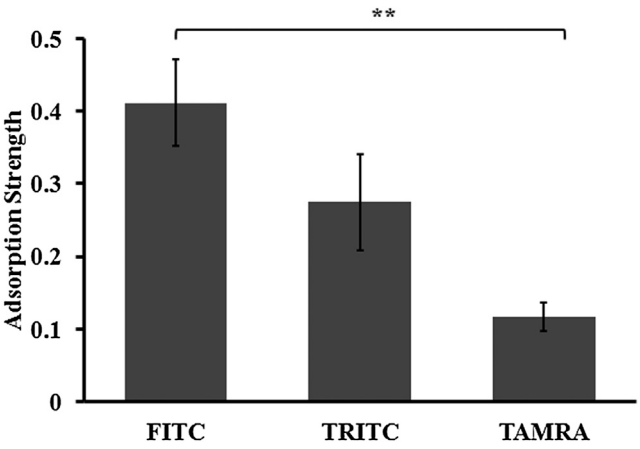

FIGURE 5 Adsorption strengths of FITC, TRITC, and TAMRA for uninjured cartilage explants. Mean ± SE ($n = 6$); ** = $p < 0.01$.

DISCUSSION

In this study, solute adsorption and distribution at the cartilage articular surface were found to differ between damaged explants (mechanically injured or sliced) and uninjured controls, as well as between fissures and adjacent intact tissue in individual damaged explants. Sliced explants were used as a positive control for mechanical injury. Living cartilage was used, therefore results may be attributed to solute-matrix and surface interactions in the presence of metabolically active cells. Surface adsorption was found to be significantly less at surface fissure sites of injured and sliced tissue compared to adjacent intact surfaces and the surface of uninjured tissue for all solutes studied, whereas effective partition coefficients were found to be unaffected by injury, suggesting that solute-surface interactions may be more sensitive indicators of tissue damage than bulk partitioning.

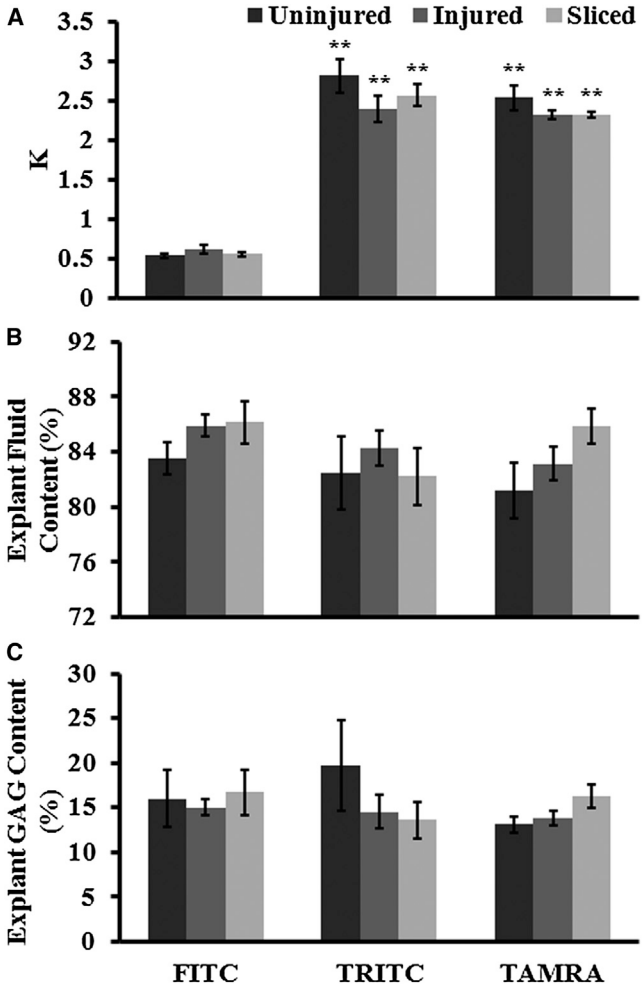

FIGURE 6 (*A*) Partition coefficients (K) of solutes within cartilage explants that were uninjured controls ($n = 5$), mechanically injured ($n = 6$), or sliced ($n = 6$). (*B*) Explant fluid content measured as fluid weight/explants wet weight (g/g) and (*C*) GAG content measured as explant total GAG weight/explant dry weight (mg/mg) of cartilage explants that were uninjured controls ($n = 6$), mechanically injured ($n = 7$), or sliced ($n = 6$). Significance represents solutes compared to FITC for each condition. Mean ± SE ($n = 6$); ** = $p < 0.01$.

The significant trend of decreased fluorescence intensity at fissured surfaces of damaged explants compared to surfaces of uninjured explants demonstrated by all solutes suggests important differences between fissured and uninjured surfaces that affect the properties of solute adsorption. This may reflect the variation of structure and biochemical composition throughout cartilage, which is divided into three distinct zones of organization. The superficial zone comprises the upper 10–20% of cartilage and can be subdivided into two layers: the first is a thin (~4–8 μm thick), proteinaceous, acellular layer of collagen fibrils termed the lamina splendens (5,34), whereas the second consists of flattened chondrocytes, densely packed collagen fibers with a relatively low proteoglycan (PG) content (35). The middle zone makes up 40–60% of cartilage and has fewer chondrocytes but a much greater PG content and the deep zone has very few cells and a lower PG content than the middle zone. Previous studies have shown that the mechanical injury protocol used in this study typically induces fissures that extend no deeper than 100–200 μm and thus are still within the superficial zone (31). Therefore, it is most probable that where fissures were present, solutes interacted with the second layer of the superficial zone. The absence of the lamina splendens in fissures may lead to changes in composition, which negatively affect solute adsorption compared to uninjured surfaces and adjacent intact surfaces. It should be noted that experimental design emphasized diffusion perpendicular to the articular surface, but in the presence of fissures there may have been significant contributions from diffusion perpendicular to the surface and through fissured surfaces. However, this should not have strongly affected the equilibrium distribution of solute.

Differences in solute adsorption between fissured surfaces and adjacent intact surfaces within individual damaged explants were evident from mean intensity ratios, which were significantly less than one for all solutes. Presumably, based upon present observations, dividing the fluorescence intensities of any two points on a healthy, uninjured cartilage articular surface would result in a mean value close to one, with smooth variation from point to point along the surface. Present results suggest that abrupt changes in surface fluorescence intensities along an articular surface (when exposed to solutes similar to those used in this study) might indicate sites of focal injury. Future work could address this correlation to assess the extent to which spatial variations in fluorescence intensity ratios provide an accurate indicator of the severity of focal injuries. These findings may therefore have clinical application. In vivo fluorescence imaging is a current area of interest that resembles fluorescence microscopy but at the tissue level. The basis of this technique is centered on selection of a fluorophore, which interacts with the bulk tissue such that changes in its structure or composition are detectable (36,37). Further advances in this technology could lead to minimally invasive cartilage imaging techniques based on fluorescence. Alternatively, currently available handheld probes for arthroscopic assessment of cartilage surfaces could be modified to detect fluorescence, allowing for identification of fissures caused by injury.

Interestingly, after desorption, fluorescence intensities of intact surfaces of damaged explants tended to be significantly higher than surfaces of uninjured explants for all solutes. This indicates that both mechanical injury and slicing induced changes in solute-surface interactions at surfaces somewhat displaced from the site of fissures. It was naively expected that intact surfaces of damaged explants would exhibit behavior similar to uninjured surfaces; thus, this discrepancy suggests that properties of the intact surface were also altered during injury. Injury is associated with a number of changes within cartilage including chondrocyte

death and altered biological activities of surviving cells, disruption of the collagen network, and changes in ECM composition (38–40). Chondrocytes that survive injury secrete degradative (and other) factors, which presumably contribute to tissue remodeling as part of a repair response (6,29,41,42). Live cartilage was used for these studies; therefore, it is possible that these secreted factors were present and, combined with matrix disruptions, affected the characteristics of the intact cartilage surface near sites of fissures. Consequently, chemical interactions and solute adsorption properties may have also been affected. Results from this study suggest that the articular surface has a higher affinity for negatively charged solutes than those that are positively charged.

Solutes used in this study exhibited adsorption strengths that seemed inconsistent with findings from previous work (27); however, these discrepancies may have been due to different explant preparation techniques, cell viabilities, and bath solutions. In this study, solutes exhibited a range of adsorption strengths, with FITC adsorbing most strongly and TAMRA most weakly. A previous study involving cartilage explants from which the superficial zone had been removed (27) exhibited opposite trends. This discrepancy may have been due to the presence or absence of the superficial zone, which is relatively poor in GAGs and associated fixed negative charge as compared to the middle zone. In this study, where the superficial zone was present, negatively charged solutes (FITC) were found to adsorb most strongly to the cartilage surface, although this trend was reversed in previous work where adsorption to the GAG-rich middle zone was measured. In addition to these electrostatic effects, this study differed from previous work (27) in that viable cartilage was used and culture media was used as bathing solution (rather than dead cartilage in PBS). Therefore, cell metabolic activities may have contributed to solute-surface interactions, whereas competitive binding interactions between fluorophores, proteins in culture media, and cartilage surfaces may have played a role as well (25).

Although effective partition coefficients (K) were slightly different from prior findings, which have reported $K>1$ for the solutes studied, the trend of partition coefficient variation between solutes was consistent with those studies (21,43–45). Previous studies that examined dead cartilage with the superficial zone removed have found $K>1$ for all solutes where $K\approx 2$ for FITC, $K\approx 5$ for TRITC, and $K\approx 1.75$ for TAMRA. As was true for solute adsorption strengths, the slight differences that did appear between partition coefficients measured in this study versus previous work (21,43–45) may be interpreted in light of different explant dissection methods, cell viability, and protein-rich culture medium. It is reasonable to expect that steric and electrostatic interactions between solute molecules and cartilage ECM largely determine K (46,47). Therefore, it should be expected that all solutes used in this study, being similar in size, would experience the same steric interactions and therefore differences in K were mainly a result of electrostatic interactions. Present results follow this logic with negatively charged FITC having $K<1$, whereas positively charged TRITC and TAMRA had $K>1$. Also consistent with previous findings (21), effective partition coefficients of solutes were not significantly affected by mechanical injury.

The specific interactions between the fluorophores of this study and cartilage surfaces involve steric, electrostatic, and other effects that are difficult to assess quantitatively. However, there is ample evidence to suggest that solute-surface interactions could be manipulated for development of cartilage-specific contrast agents. For example, though TRITC and TAMRA both have the same charge and approximately the same size, they exhibit somewhat different adsorption properties (27). This difference may be related to subtle differences in their functional groups; both have the same base structure however TAMRA has a carboxyl (-COOH) group where TRITC has an isothiocyanate (-N=C=S) group. Therefore, relatively simple chemical modifications may be sufficient to tune a solute's interactions with cartilage surfaces. There are numerous possibilities for conjugation of molecular groups to solutes and further experiments would provide increased insight into ways of manipulating solute interactions with fissured and uninjured cartilage surfaces. Conjugation of fluorescent solutes or other image contrast agents to molecular groups, which exhibit selective binding to either intact articular surfaces or to fissures, could lead to a sensitive minimally invasive indicator of focal injuries. For example, lubricin is a glycoprotein secreted by chondrocytes in the superficial zone, which binds to the articular surface through its C-terminal domain; therefore, it may lead to a prominent signal at intact surfaces versus fissures (48). Additionally, peptide sequences that show a strong binding affinity for chondrocytes present a variety of options to investigate preferential binding to fissures where chondrocytes are exposed (49).

CONCLUSION

Adsorption of fluorescent solutes to fissures on the articular surface of damaged cartilage explants was significantly reduced versus adsorption to uninjured cartilage surfaces. This very clear trend was largely independent of the fluorophore used, and also did not depend upon whether the damage was induced by injurious compression or slicing. Significant differences between solute adsorption to fissures and adjacent intact cartilage within damaged explants suggested that this contrast might be useful for detection of cartilage injuries in vivo. Surprisingly, solutes were also found to adsorb more strongly to intact surfaces of injured and sliced explants than to uninjured explant surfaces, suggesting that injury not only creates fissures but also alters the surface properties of the adjacent intact tissue. Solute adsorption strengths and partition coefficients were

reasonably consistent with findings from previous studies, but some differences existed that may have been due to different explant preparation techniques, viability, and bathing solutions. Overall, results highlight the sensitivity of solute-surface interactions to tissue damage and the appearance of fissures, and suggest that these phenomena may be useful for development of cartilage-specific imaging contrast agents and more accurate minimally invasive detection of focal injuries to the articular surface.

This project was supported by the National Science and Engineering Research Council (NSERC) Discovery Grant, Canada Foundation for Innovation and Canada Research Chair programs.

The authors of this manuscript have no conflicts of interest.

REFERENCES

1. Freeman, M. A. R. 1979. Adult Articular Cartilage. Pitman Medical, Tunbridge Wells, England.
2. Becerra, J., J. A. Andrades, …, A. H. Reddi. 2010. Articular cartilage: structure and regeneration. *Tissue Eng. Part B Rev.* 16:617–627.
3. Temenoff, J. S., and A. G. Mikos. 2000. Review: tissue engineering for regeneration of articular cartilage. *Biomaterials.* 21:431–440.
4. Buckwalter, J. A. 1998. Articular cartilage: injuries and potential for healing. *J. Orthop. Sports Phys. Ther.* 28:192–202.
5. Athanasiou, K. A., E. M. Darling, and J. C. Hu. 2010. Articular Cartilage Tissue Engineering. Morgan & Claypool Publishers, San Rafael, Calif.
6. Buckwalter, J. A., and H. J. Mankin. 1997. Articular cartilage part II: degeneration and osteoarthrosis, repair, regeneration, and transplantation. *J. Bone Joint Surg. Am.* 79A:612–632.
7. Madry, H., F. P. Luyten, and A. Facchini. 2012. Biological aspects of early osteoarthritis. *Knee Surg. Sports Traumatol. Arthrosc.* 20:407–422.
8. Pearle, A. D., R. F. Warren, and S. A. Rodeo. 2005. Basic science of articular cartilage and osteoarthritis. *Clin. Sports Med.* 24:1–12.
9. Tiderius, C. J., L. E. Olsson, …, L. Dahlberg. 2003. Delayed gadolinium-enhanced MRI of cartilage (dGEMRIC) in early knee osteoarthritis. *Magn. Reson. Med.* 49:488–492.
10. Samosky, J. T., D. Burstein, …, M. L. Gray. 2005. Spatially-localized correlation of dGEMRIC-measured GAG distribution and mechanical stiffness in the human tibial plateau. *J. Orthop. Res.* 23:93–101.
11. McKenzie, C. A., A. Williams, …, D. Burstein. 2006. Three-dimensional delayed gadolinium-enhanced MRI of cartilage (dGEMRIC) at 1.5T and 3.0T. *J. Magn. Reson. Imaging.* 24:928–933.
12. Bansal, P. N., N. S. Joshi, …, B. D. Snyder. 2010. Contrast enhanced computed tomography can predict the glycosaminoglycan content and biomechanical properties of articular cartilage. *Osteoarthritis Cartilage.* 18:184–191.
13. Yoo, H. J., S. H. Hong, …, H. S. Kang. 2011. Contrast-enhanced CT of articular cartilage: experimental study for quantification of glycosaminoglycan content in articular cartilage. *Radiology.* 261:805–812.
14. Kokkonen, H. T., J. S. Jurvelin, …, J. Töyräs. 2011. Detection of mechanical injury of articular cartilage using contrast enhanced computed tomography. *Osteoarthritis Cartilage.* 19:295–301.
15. Kokkonen, H. T., J. Mäkelä, …, J. Töyräs. 2011. Computed tomography detects changes in contrast agent diffusion after collagen crosslinking typical to natural aging of articular cartilage. *Osteoarthritis Cartilage.* 19:1190–1198.
16. Taylor, C., J. Carballido-Gamio, …, X. J. Li. 2009. Comparison of quantitative imaging of cartilage for osteoarthritis: T2, T1rho, dGEMRIC and contrast-enhanced computed tomography. *Magn. Reson. Imaging.* 27:779–784.
17. Bansal, P. N., R. C. Stewart, …, M. W. Grinstaff. 2011. Contrast agent electrostatic attraction rather than repulsion to glycosaminoglycans affords a greater contrast uptake ratio and improved quantitative CT imaging in cartilage. *Osteoarthritis Cartilage.* 19:970–976.
18. Bansal, P. N., N. S. Joshi, …, M. W. Grinstaff. 2011. Cationic contrast agents improve quantification of glycosaminoglycan (GAG) content by contrast enhanced CT imaging of cartilage. *J. Orthop. Res.* 29:704–709.
19. Joshi, N. S., P. N. Bansal, …, M. W. Grinstaff. 2009. Effect of contrast agent charge on visualization of articular cartilage using computed tomography: exploiting electrostatic interactions for improved sensitivity. *J. Am. Chem. Soc.* 131:13234–13235.
20. Silvast, T. S., H. T. Kokkonen, …, J. Töyräs. 2009. Diffusion and near-equilibrium distribution of MRI and CT contrast agents in articular cartilage. *Phys. Med. Biol.* 54:6823–6836.
21. Chin, H. C., M. Moeini, and T. M. Quinn. 2013. Solute transport across the articular surface of injured cartilage. *Arch. Biochem. Biophys.* 535:241–247.
22. Schwarz, I. M., and B. A. Hills. 1998. Surface-active phospholipid as the lubricating component of lubricin. *Br. J. Rheumatol.* 37:21–26.
23. Murakami, T., K. Nakashima, …, N. Hosoda. 2009. Roles of adsorbed film and gel layer in hydration lubrication for articular cartilage. *P I Mech Eng J-J Eng.* 223:287–295.
24. Jones, A. R. C., J. P. Gleghorn, …, C. R. Flannery. 2007. Binding and localization of recombinant lubricin to articular cartilage surfaces. *J. Orthop. Res.* 25:283–292.
25. Nugent-Derfus, G. E., A. H. Chan, …, R. L. Sah. 2007. PRG4 exchange between the articular cartilage surface and synovial fluid. *J. Orthop. Res.* 25:1269–1276.
26. Gale, L. R., Y. Chen, …, R. Crawford. 2007. Boundary lubrication of joints: characterization of surface-active phospholipids found on retrieved implants. *Acta Orthop.* 78:309–314.
27. Moeini, M., and T. M. Quinn. 2012. Solute adsorption to surfaces of articular cartilage explants: apparent versus actual partition coefficients. *Soft Matter.* 8:11880–11888.
28. Morel, V., and T. M. Quinn. 2004. Cartilage injury by ramp compression near the gel diffusion rate. *J. Orthop. Res.* 22:145–151.
29. Rosenzweig, D. H., M. J. Djap, …, T. M. Quinn. 2012. Mechanical injury of bovine cartilage explants induces depth-dependent, transient changes in MAP kinase activity associated with apoptosis. *Osteoarthritis Cartilage.* 20:1591–1602.
30. Morel, V., and T. M. Quinn. 2004. Short-term changes in cell and matrix damage following mechanical injury of articular cartilage explants and modelling of microphysical mediators. *Biorheology.* 41:509–519.
31. Morel, V., C. Berutto, and T. M. Quinn. 2006. Effects of damage in the articular surface on the cartilage response to injurious compression in vitro. *J. Biomech.* 39:924–930.
32. Evans, R. C., and T. M. Quinn. 2006. Dynamic compression augments interstitial transport of a glucose-like solute in articular cartilage. *Biophys. J.* 91:1541–1547.
33. Farndale, R. W., C. A. Sayers, and A. J. Barrett. 1982. A direct spectrophotometric microassay for sulfated glycosaminoglycans in cartilage cultures. *Connect. Tissue Res.* 9:247–248.
34. Teshima, R., T. Otsuka, …, K. Yamamoto. 1995. Structure of the most superficial layer of articular cartilage. *J. Bone Joint Surg. Br.* 77:460–464.
35. Buckwalter, J. A., H. J. Mankin, and A. J. Grodzinsky. 2005. Articular cartilage and osteoarthritis. *Instr. Course Lect.* 54:465–480.
36. Andersson-Engels, S., C. Klinteberg, …, S. Svanberg. 1997. In vivo fluorescence imaging for tissue diagnostics. *Phys. Med. Biol.* 42:815–824.
37. Rao, J., A. Dragulescu-Andrasi, and H. Yao. 2007. Fluorescence imaging in vivo: recent advances. *Curr. Opin. Biotechnol.* 18:17–25.
38. Démarteau, O., L. Pillet, …, T. M. Quinn. 2006. Biomechanical characterization and in vitro mechanical injury of elderly human femoral

head cartilage: comparison to adult bovine humeral head cartilage. *Osteoarthritis Cartilage.* 14:589–596.

39. D'Lima, D. D., S. Hashimoto, …, M. K. Lotz. 2001. Impact of mechanical trauma on matrix and cells. *Clin. Orthop. Relat. Res.* 403(*Suppl*):S90–S99.
40. Quinn, T. M., R. G. Allen, …, E. B. Hunziker. 2001. Matrix and cell injury due to sub-impact loading of adult bovine articular cartilage explants: effects of strain rate and peak stress. *J. Orthop. Res.* 19:242–249.
41. Pickvance, E. A., T. R. Oegema, Jr., and R. C. Thompson, Jr. 1993. Immunolocalization of selected cytokines and proteases in canine articular cartilage after transarticular loading. *J. Orthop. Res.* 11:313–323.
42. Quinn, T. M., A. A. Maung, …, J. D. Sandy. 1999. Physical and biological regulation of proteoglycan turnover around chondrocytes in cartilage explants. Implications for tissue degradation and repair. *Ann. N. Y. Acad. Sci.* 878:420–441.
43. Moeini, M., K. B. Lee, and T. M. Quinn. 2012. Temperature affects transport of polysaccharides and proteins in articular cartilage explants. *J. Biomech.* 45:1916–1923.
44. Quinn, T. M., V. Morel, and J. J. Meister. 2001. Static compression of articular cartilage can reduce solute diffusivity and partitioning: implications for the chondrocyte biological response. *J. Biomech.* 34:1463–1469.
45. Quinn, T. M., P. Kocian, and J. J. Meister. 2000. Static compression is associated with decreased diffusivity of dextrans in cartilage explants. *Arch. Biochem. Biophys.* 384:327–334.
46. Maroudas, A. 1970. Distribution and diffusion of solutes in articular cartilage. *Biophys. J.* 10:365–379.
47. Maroudas, A., P. D. Weinberg, …, C. P. Winlove. 1988. The distributions and diffusivities of small ions in chondroitin sulphate, hyaluronate and some proteoglycan solutions. *Biophys. Chem.* 32:257–270.
48. Bao, J. P., W. P. Chen, and L. D. Wu. 2011. Lubricin: a novel potential biotherapeutic approaches for the treatment of osteoarthritis. *Mol. Biol. Rep.* 38:2879–2885.
49. Ruoslahti, E. 1996. RGD and other recognition sequences for integrins. *Annu. Rev. Cell Dev. Biol.* 12:697–715.